ACS Medicinal Chemistry Letters

Letter

pubs.acs.org/acsmedchemlett

Discovery of a Potent Parenterally Administered Factor XIa Inhibitor with Hydroxyquinolin-2(1*H*)-one as the P2′ Moiety

Zilun Hu,* Pancras C. Wong, Paul J. Gilligan, Wei Han, Kumar B. Pabbisetty, Jeffrey M. Bozarth, Earl J. Crain, Timothy Harper, Joseph M. Luettgen, Joseph E. Myers, Jr., Vidhyashankar Ramamurthy, Karen A. Rossi, Steven Sheriff, Carol A. Watson, Anzi Wei, Joanna J. Zheng, Dietmar A. Seiffert, Ruth R. Wexler, and Mimi L. Quan

Research and Development, Bristol-Myers Squibb, Princeton, New Jersey 08543, United States

Supporting Information

ABSTRACT: Structure–activity relationship optimization of phenylalanine P1′ and P2′ regions with a phenylimidazole core resulted in a series of potent FXIa inhibitors. Introducing 4-hydroxyquinolin-2-one as the P2′ group enhanced FXIa affinity and metabolic stability. Incorporation of an *N*-methyl piperazine amide group to replace the phenylalanine improved both FXIa potency and aqueous solubility. Combination of the optimization led to the discovery of FXIa inhibitor **13** with a FXIa K_i of 0.04 nM and an aPTT EC_{2x} of 1.0 μM. Dose-dependent efficacy (EC_{50} of 0.53 μM) was achieved in the rabbit ECAT model with minimal bleeding time prolongation.

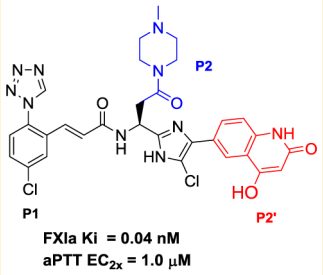

KEYWORDS: *Thrombosis, factor XIa, anticoagulant*

Thrombosis remains a primary cause of cardiovascular morbidity and mortality. The established anticoagulants, such as injectable heparin and warfarin, suffer from enhanced risk of bleeding and narrow therapeutic index.[1−3] The newer anticoagulants, including apixaban, rivaroxaban, edoxaban, and dabigatran, primarily target direct factor Xa (FXa) or thrombin inhibition, respectively, which belong to the common pathway in the coagulation cascade. These agents have shown an improved efficacy and bleeding safety profile.[4−9] Factor XIa (FXIa) is positioned upstream in the coagulation cascade and is involved in the amplification of thrombin production. Genetic evidence suggests FXIa could be an antithrombotic target with net clinical benefit.[10] FXI deficient mice do not exhibit prolonged provoked bleeding times.[11−13] Deficiency of human FXI is only associated with a mild bleeding diathesis. Inhibiting FXIa could provide a reduction in thrombin to a level sufficient to impede occlusive thrombosis, yet allow enough thrombin generation to support hemostasis.[14] Inhibition of FXIa has been demonstrated to be a viable antithrombotic approach with an improved benefit to risk ratio in preclinical animal models,[15,16] and recently in a clinical phase II proof of concept study with FXIa antisense oligonucleotide,[17] with minimal effects on provoked bleeding time.

We have reported a reversible, small molecule FXIa inhibitor with a tetrahydroquinoline core (**1**, Figure 1), which demonstrated antithrombotic efficacy without prolonging bleeding time in rabbit antithrombotic efficacy and bleeding models.[18,19] We have also reported the discovery of a series of potent FXIa inhibitors (**2**) containing a phenylimidazole core.[20] Structure–activity relationship (SAR) efforts to replace basic

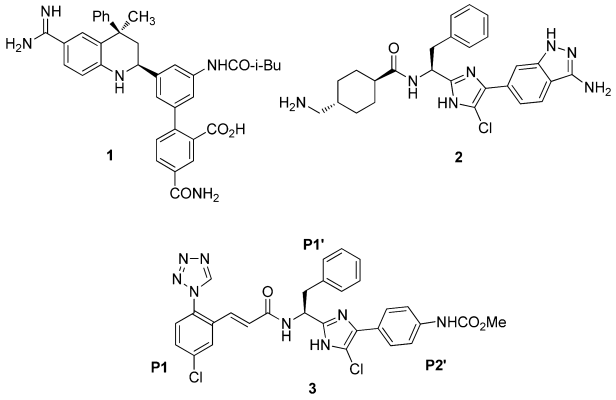

Figure 1. FXIa inhibitors previously reported by our group.

1,4-tranexamic amide P1 in compound **2** identified neutral FXIa inhibitor **3**.[21] Compound **3** has a K_i 3.7 nM in the FXIa enzyme binding assay. It exhibits an EC_{2x} of 19 μM *in vitro* anticoagulant activity in the activated partial thromboplastin time (aPTT) clotting assay. Herein, we describe the continued SAR optimization at the phenylalanine P1 prime (P1′) and P2 prime (P2′) regions with compound **3** to further improve potency, stability, and solubility toward the discovery of a potent and efficacious parenteral FXIa inhibitor.

Received: February 5, 2015
Accepted: April 8, 2015
Published: April 8, 2015

DOI: 10.1021/acsmedchemlett.5b00066
ACS Med. Chem. Lett. 2015, 6, 590−595

Possible cleavage of the P2′ methylcarbamate in **3** to release an aniline moiety was envisioned to be a potential safety issue. One of the approaches to optimize P2′ was to utilize tied-back fused ring systems to replace the aniline methyl carbamate. As shown in Table 1, changing P2′ from methyl carbamate in **3** to dihydroquinolinone in **4** and quinolinone in **5** retained most of the FXIa enzyme binding and *in vitro* anticoagulant aPTT clotting potencies. From molecular modeling, it was envisioned that additional affinity could be achieved by the interaction between the quinolinone moiety and tyrosine 143 (Tyr 143) of the enzyme. Indeed, introducing a hydroxyl group at the 4-position of quinolinone, such as in analogues **6** and **7**, improved both FXIa binding and aPTT potency significantly with FXIa K_i of 0.5 and 0.32 nM, and aPTT EC_{2x} of 9.1 and 7.2 μM, respectively. Human liver microsome half-life assay indicated the analogues with ethylene linker, such as **5**, **6**, and **7** of the P1 groups, had poor metabolic stability. Incorporation of the ethenyl linker in compound **8** improved FXIa K_i (0.18 nM) while having similar aPTT (EC_{2x} 11 μM) potency and improved human liver microsome half-life.

Table 1. P2′ Tied-Back SAR

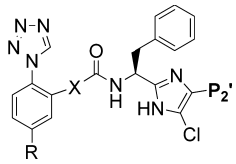

Entry	P2′	X	R	FXIa Ki[a] (nM)	aPTT EC_{2x}[b] (μM)	HLM $T_{1/2}$[c] (min)
3	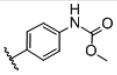		Cl	3.7	19	46
4	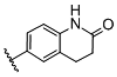		Cl	19	60	48
5	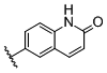		Me	12	69	2.2
6	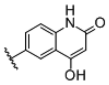		Me	0.5	9.1	10
7	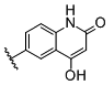		Cl	0.32	7.2	6.6
8	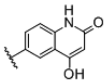		Cl	0.18	11	56

[a]K_i values were obtained from human enzyme and were averaged from multiple determinations (n = 2), as described in ref 20. [b]Activated partial thromboplastin time (aPTT) *in vitro* clotting assay was performed in human plasma, as described in ref 20. [c]Human liver microsome half-life (HLM $T_{1/2}$) of compounds were determined by following the method described in ref 22.

Phenylalanine replacement SAR was explored to improve *in vitro* anticoagulant activity and aqueous solubility by the incorporation of polar groups. As listed in Table 2, changing the R group from analogue of phenyl alanine (**3**) to aspartate analogue of morpholine amide (**9**) afforded a very potent inhibitor with a FXIa K_i of 0.7 nM and an aPTT EC_{2x} of 7.4 μM. The X-ray crystal structure[23] (Figure 2) indicated that **9** bound to the FXIa active site with the chlorophenyl tetrazole fit in the S1 pocket having an edge-to-face interaction between the chlorophenyl and Tyr 228. The carbonyl of the acrylamide formed hydrogen bond interactions with the backbone NH of residues Gly 193 and Ser 195, which form part of the oxyanion hole. The nitrogen of the acrylamide made a hydrogen bond via a water to the backbone carbonyl of Ser 214. The 3-nitrogen of the imidazole formed a hydrogen bond through a water to Leu 41 carbonyl and the OH of Ser 195. The chlorine formed a lipophilic interaction with the side chain of Lys 192. The phenyl methyl carbamate bound in the S2′ pocket and the nitrogen formed a hydrogen bond with the backbone carbonyl of His 40. The structure showed that the morpholine ring projected toward the S2 pocket and differs from the benzyl group in compound **3**, which projected into the S1′ pocket. The P2 linker carbonyl made a hydrogen bond to Leu 41.

Table 2. SAR of Aspartate Amide Analogues

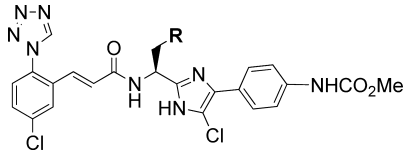

Entry	R	FXIa Ki[a] (nM)	aPTT EC_{2x}[b] (μM)	Solubility[c] (μg/mL)	HLM $T_{1/2}$[d] (min)
3		3.7	19	<1	46
9		0.7	7.4	1	6.2
10	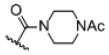	0.6	4.6	3	45
11	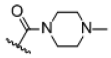	0.4	3.7	44	25
12	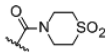	0.3	3.6	1	154

[a]K_i values were obtained from human enzyme and were averaged from multiple determinations (n = 2), as described in ref 20. [b]Activated partial thromboplastin time (aPTT) *in vitro* clotting assay was performed in human plasma, as described in ref 20. [c]Amorphous, 50 mM pH 6.5 phosphate buffer. [d]Human liver microsome half-life (HLM $T_{1/2}$) of compounds were determined by following the method described in ref 22.

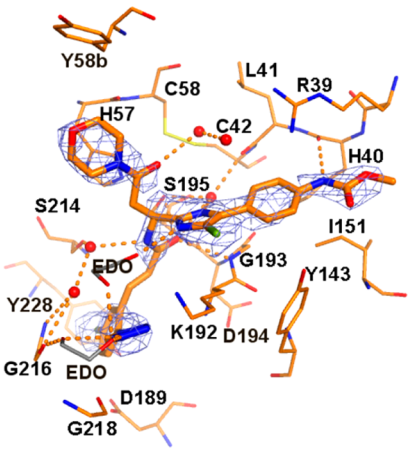

Figure 2. X-ray crystal structure of **9** in FXIa. Final model is shown with initial Fo-Fc map contoured at 2.5 rmsd. Hydrogen bonds are shown as a series of prolate ellipsoids.

DOI: 10.1021/acsmedchemlett.5b00066
ACS Med. Chem. Lett. 2015, 6, 590−595

Unfortunately, inhibitor **9** did not show improvement in solubility or human liver microsome stability. The analogue of 4-acetylpiperazine amide (**10**) maintained excellent FXIa binding and anticoagulation potency (FXIa K_i 0.6 nM and aPTT EC_{2x} 4.6 μM). With the incorporation of a more basic methyl piperazine, analogue **11** not only demonstrated excellent enzyme affinity (FXIa K_i 0.4 nM) and *in vitro* anticoagulant potency (aPTT EC_{2x} 3.7 μM) but also enhanced aqueous solubility (44 μg/mL). The corresponding thiomorpholine 1,1-dioxide analogue **12** had excellent FXIa affinity (FXIa K_i 0.3 nM), *in vitro* anticoagulant potency (aPTT EC_{2x} 3.6 μM), and significant improvement of human liver microsome stability, but unfortunately no increase in solubility.

Further SAR efforts to combine the P2′ hydroxyquinolinone group in **8** and the P2 *N*-methylpiperazine amide in **11** into one molecule (**13**) demonstrated additive effects on the FXIa affinity and *in vitro* anticoagulation aPTT potency (Figure 3).

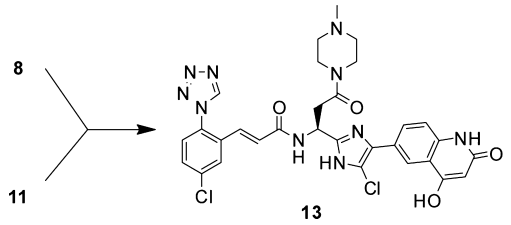

Figure 3. Combination of P2 and P2′ SAR.

Compound **13** has a FXIa K_i of 0.04 nM and an aPTT EC_{2x} of 1.0 μM, with aqueous solubility of 17 μg/mL in pH 6.5 buffer. In human liver microsome, **13** has a half-life measured at >200 min.

An X-ray crystal structure (Figure 4A) of compound **13** bound in the active site of FXIa was obtained at 2.2 Å resolution.[23] Similar to compound **9**, the X-ray structure showed that the chlorophenyltetrazole moiety occupied the S1 pocket. Additionally, the carbonyl of the acrylamide formed hydrogen bond interactions with the oxyanion hole, and the 3-nitrogen of the ring formed a hydrogen bond with Ser 195 OH and Leu 41 carbonyl through a water. The *N*-methyl piperazine bound above His 57 and was flanked by Tyr 58B in the P2 pocket.

In the S2′ region, both the NH and carbonyl of quinolinone formed hydrogen bonds with His 40, while the OH formed a hydrogen bond with Tyr 143. Figure 4B shows the superimposition comparison of the X-ray crystal structure of compound **13** with compound **3**[23] bound in the active site of FXIa. The two compounds show a similar binding mode, with extra interactions observed from the P2 and P2′ regions for compound **13**.

A representative synthesis of the P2′ analogues in Table 1 is illustrated in Scheme 1 (see Supporting Information). Condensation of *N*-Boc-L-phenylalaninal **1a** and glyoxal trimer with ammonia in methanol afforded 4,5-unsubstituted imidazole **1b**. Monochlorination with NCS, followed by bromination with NBS, afforded 4-bromo-5-chloro imidazole derivative **1c**. Suzuki−Miyaura coupling of **1c** with boronic acid **1e**, which was prepared from **1d**,[24] gave quinolinone amine derivative **1f** after removal of the Boc group. Amide formation of **1f** with **1g**[21] afforded **5**.

Compound **13** was prepared following the procedure described in Scheme 2. The imidazole intermediate **2b** was prepared by following a modified procedure as reported in

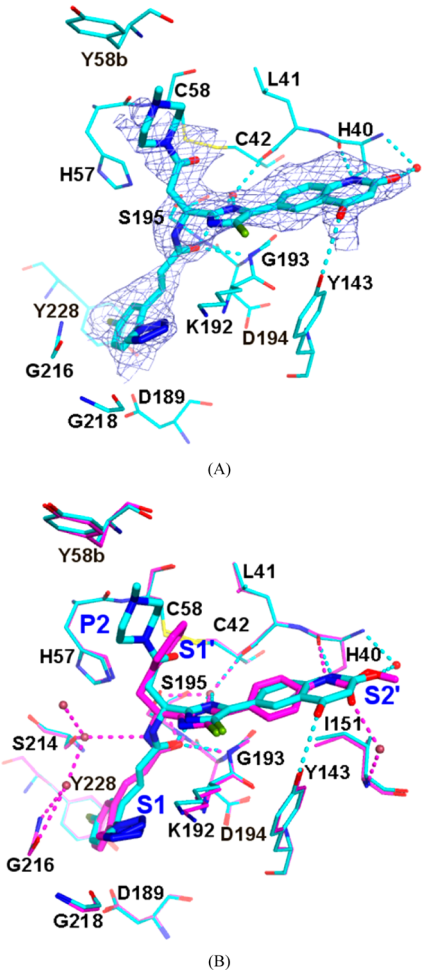

Figure 4. (A) X-ray crystal structure of **13** in FXIa. Final model is shown with initial Fo-Fc electron density contoured at 2.5 rmsd. The high B-factors of compound **13** in the final model suggest that it has only partially occupied the site. As a consequence, a relatively low contour level is needed, and the chlorine of the chloroimidazole is not covered with density. (B) X-ray structure of **13** (cyan) superimposed with the X-ray structure of **3** (magenta).

literature.[25] The alkylation of *N*-Boc phenylalanine with 2-bromo-1-(4-nitrophenyl) gave α-acyloxyketone **2a**, which underwent cyclization to form 4-arylimidazole **2b** by heating with NH_4OAc in xylene. Chlorination at the C5 position with NCS afforded **2c**. Reducing the nitro group afforded amine **2d**, which was coupled with malonic acid mono-*tert*-butyl ester to provide **2e**. Cyclization of **2e** under heating PPA conditions provided 4-hydroxyquinolinone amino acid **2f** in near quantitative yield. This amino acid was reacted with *N*-hydroxysuccinimide ester **2h**, which was prepared from **2g**,[21] to give the penultimate acid **2i**. Final amide coupling under mixed anhydride conditions afforded **13** in good overall yield (26%).

Compound **13** was highly selective against other related serine proteases except plasma kallikrein[26] with a K_i of 7 nM (Table 3). The *in vitro* and *in vivo* profiles of compound **13**, including enzyme binding, anticoagulation aPTT potency, plasma protein binding, and pharmacokinetics across different species, are summarized in Table 4. Compound **13** has a very good human *in vitro* profile and, in addition, has a similar FXIa affinity and aPTT in rabbit, the species used for animal modeling, with a K_i of 0.58 nM and $EC_{1.5x}$ of 1.0 μM in rabbit, respectively. Compound **13** demonstrated high free fractions in

DOI: 10.1021/acsmedchemlett.5b00066
ACS Med. Chem. Lett. 2015, 6, 590−595

Scheme 1[a]

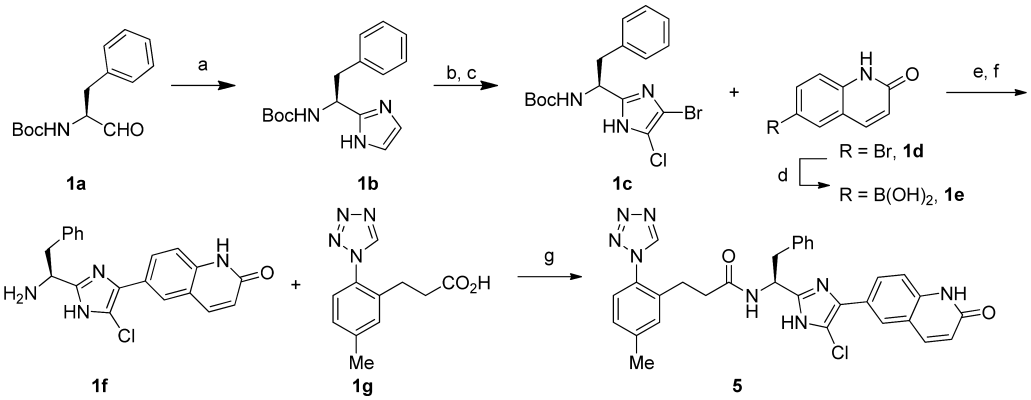

[a]Reagents and conditions: (a) glyoxal trimer dihydrate, 7 N NH_3 in MeOH, rt, 70%; (b) NCS, CH_3CN, 0−50 °C, 36%; (c) NBS, $CHCl_3$, rt, 71%; (d) bis(neopentylglycolato)diboron, $PdCl_2$(dppf), KOAc, DMSO, 85%; (e) Pd(t-Bu_3P)$_2$, K_3PO_4, dioxane/H_2O, 80 °C, 78%; (f) TFA, DCM, 100%; (g) EDC, HOBt, DIEA, DMF, 44%.

Scheme 2[a]

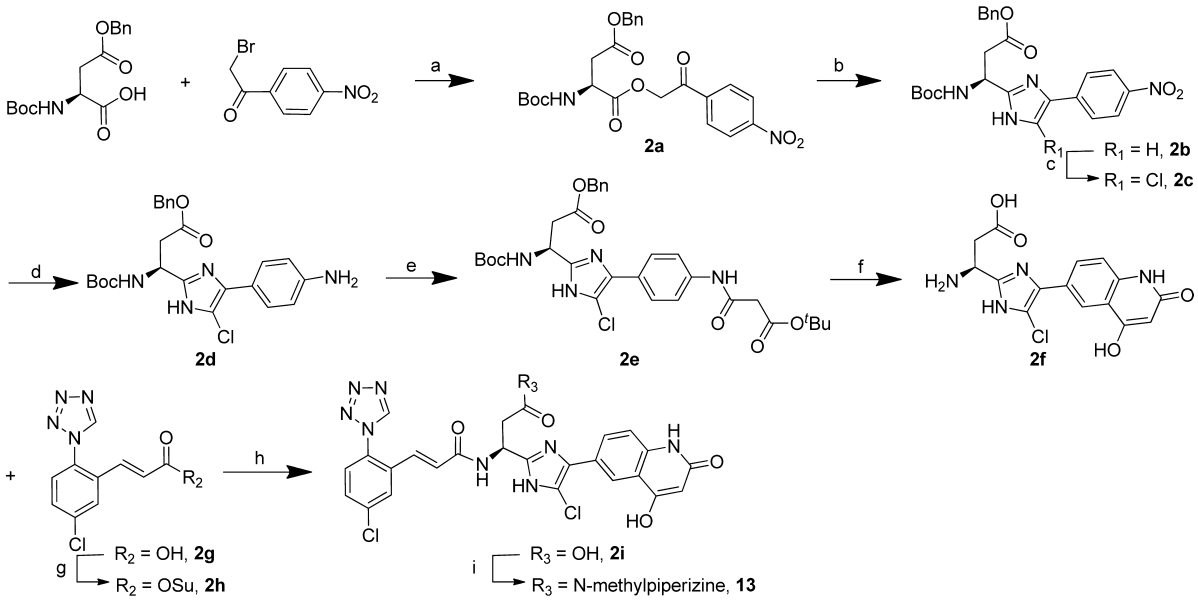

[a]Reagents and conditions: (a) Cs_2CO_3, 30 min, rt, 94%; (b) NH_4OAc, xylene, reflux, 77%; (c) NCS, MeCN, 70 °C, 80%; (d) $SnCl_2$, NH_4Cl, MeOH, 98%; (e) PyBOP, DIEA, DMF, 91%; (f) PPA, 130 °C, >95%; (g) N-hydroxysuccinimide, DIC, DMF, rt, 100%; (h) DIEA, DMSO, 89%; (i) isobutylchloroformate, DIEA, DMF, 0 °C, 5 min, then N-methylpiperazine, 0 °C, 57%.

Table 3. Selectivity of Compound 13 against Related Enzymes

H. enzyme	FXIa	FVIIa	FXa	FIXa	FXIIa	thrombin	trypsin	P. kallikrein	T. kallikrein	chrymotripsin	tPA	urokinase	APC
K_i^a (nM)	0.04	>13330	>9000	>60000	>20000	7400	6200	7.0	>30000	400	29000	>1600	>54000

[a]K_i values were obtained from human enzyme and were averaged from duplicated IC_{50} determinations.

plasma protein binding studies across the species evaluated, with 8% free for human and cyno, 7% for rabbit, and 18% for dog. In pharmacokinetics studies, the half-life was shown to be suitable for *iv* administration (1 to 2 h across all species).

Compound **13** was evaluated in the rabbit electrically induced carotid arterial thrombosis (ECAT) model.[27] As shown in Figure 5, **13** produced a dose-dependent increase in integrated blood flow of the injured artery. A dose-dependent increase in potency of thrombus reduction is demonstrated in the antithrombotic concentration−response curve in the rabbit ECAT with an EC_{50} of 0.53 μM (Figure 6). In the rabbit cuticle bleeding time (CBT) model,[28] only minimal bleeding time prolongation was observed for **13** even at the highest dose studied, as indicated in the bleeding time curve shown in Figure 6. At the top dose, **13** prolonged aPTT by 3.2-fold, but not prothrombin time (PT) or thrombin time (TT), as expected with the FXIa mechanism.

In summary, optimization of an imidazole series of FXIa inhibitors at the P2 and P2′ regions led to the discovery of a potent inhibitor **13** with a FXIa K_i of 0.04 nM, an aPTT $EC_{1.5x}$ of 0.28 μM, and a short half-life suitable for parenteral dosing. Compound **13** demonstrated robust antithrombotic efficacy in

DOI: 10.1021/acsmedchemlett.5b00066
ACS Med. Chem. Lett. 2015, 6, 590−595

Table 4. Profile of Compound 13 in Different Species

	human	rabbit	dog	rat	cyno
XIa K_i^a (nM)	0.10	0.58			
aPTT $EC_{1.5x}$ (μM)	0.28	1.0	0.3	>20	0.3
free fraction (%)	8.0	7.0	18	2.6	8.0
PK half-life^b (h)		1.1	1.1	1.1	1.9

^{a}Determined at 37 °C. ^{b}IV dosed at 1 mg/kg. Salt forms and formulations: rabbit, **13**-HCl salt, 10% DMAc/90% D5W (5% dextrose in water); dog, **13**-HCl salt, 10% DMAc/10% ethanol/10% propylene glycol/70% water; rat, **13**-TFA salt, 10% DMAc/90% water; cyno, **13**-HCl salt, 10% DMAc/90% water.

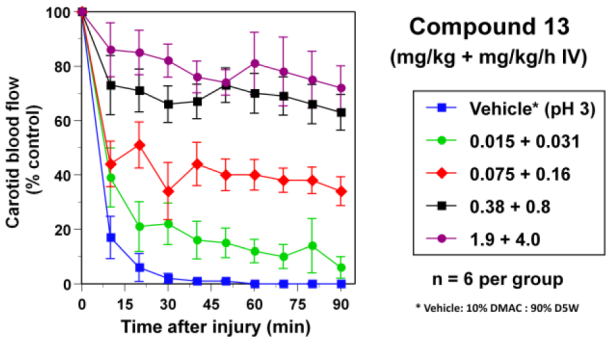

Figure 5. Antithrombotic effect of compound **13** in rabbit ECAT model.

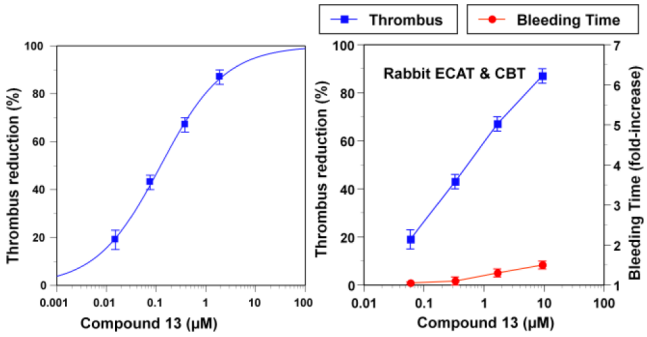

Figure 6. Compound **13** in rabbit ECAT efficacy and CBT bleeding models. (A) Antithrombotic concentration−response curve in the rabbit ECAT. (B) Antithrombotic efficacy (blue) vs bleeding time (red).

a rabbit ECAT thrombosis model with an EC_{50} of 0.53 μM. In the rabbit CBT model, minimal increase in bleeding time was observed. Overall, the favorable profile of compound **13** allowed further preclinical evaluation to determine its potential as a parenteral antithrombotic agent.

■ ASSOCIATED CONTENT

Supporting Information

Experimental procedures and characterization data for compounds **4**−**13**. This material is available free of charge via the Internet at http://pubs.acs.org.

■ AUTHOR INFORMATION

Corresponding Author

*E-mail: zilun.hu@bms.com. Tel: (1) 609-818-5290.

Notes

The authors declare no competing financial interest.

■ ACKNOWLEDGMENTS

We thank Dr. Ying Han for generation of a P2 compound library, and the Department of Discovery Synthesis and BMS Biocon Research Center for the large-scale synthesis of intermediate **1c**. Use of the Advanced Photon Source was supported by the U.S. Department of Energy, Office of Science, Office of Basic Energy Sciences, under Contract No. DE-AC02-06CH11357, and use of the IMCA-CAT beamline 17-BM at the Advanced Photon Source was supported by the companies of the Industrial Macromolecular Crystallography Association through a contract with Hauptman-Woodward Medical Research Institute.

■ REFERENCES

(1) Ansell, J.; Hirsh, J.; Hylek, E.; Jacobson, A.; Crowther, M.; Palareti, G. Pharmacology and management of the vitamin K antagonists: American College of Chest Physicians Evidence-based Clinical Practice Guidelines (8th Edition). *Chest* **2008**, *133*, 160S−198S.

(2) Stein, P. D.; Grandison, D.; Hua, T. A. Therapeutic level of anticoagulation with warfarin in patients with mechanical prosthetic heart valves: review of literature and recommendations based on internal normalized ratio. *Postgrad. Med. J.* **1994**, *70* (suppl 1), S72−S83.

(3) Hirsh, J.; Poller, L. The international normalized ratio. A guide to understanding and correcting its problems. *Arch. Int. Med.* **1994**, *154*, 282−288.

(4) Yeh, C. H.; Fredenburgh, J. C.; Weitz, J. I. Oral direct factor Xa inhibitors. *Circ. Res.* **2012**, *111* (8), 1069−1078.

(5) Spinler, S. The pharmacology and therapeutic use of dabigatran etexilate. *J. Clin. Pharmacol.* **2013**, *53* (1), 1−13.

(6) Pinto, D. J. P.; Wong, P. C.; Knabb, R. M.; Wexler, R. R. Case history: Eliquis (Apixaban), a potent and selective inhibitor of coagulation factor Xa for the prevention and treatment of thrombotic diseases. *Annu. Rep. Med. Chem.* **2012**, *47*, 123−139.

(7) Granger, C. B.; Alexander, J. H.; McMurray, J. J.; Lopes, R. D.; Hylek, E. M.; Hanna, M.; Al-Khalidi, H. R.; Ansell, J.; Atar, D.; Avezum, A.; Bahit, M. C.; Diaz, R.; Easton, J. D.; Ezekowitz, J. A.; Flaker, G.; Garcia, D.; Geraldes, M.; Gersh, B. J.; Golitsyn, S.; Goto, S.; Hermosillo, A. G.; Hohnloser, S. H.; Horowitz, J.; Mohan, P.; Jansky, P.; Lewis, B. S.; Lopez-Sendon, J. L.; Pais, P.; Parkhomenko, A.; Verheugt, F. W.; Zhu, J.; Wallentin, L. Apixaban versus warfarin in patients with atrial fibrillation. *N. Engl. J. Med.* **2011**, *365* (11), 981−992.

(8) Perzborn, E.; Roehring, S.; Straub, A.; Kubitza, D.; Misselwitz, F. The discovery and development of rivaroxaban, an oral, direct factor Xa inhibitor. *Nat. Rev. Drug Discovery* **2011**, *10*, 61−75.

(9) Straub, A.; Roehrig, S.; Hillisch, A. Entering the era of non-basic P1 site groups: discovery of Xarelto (Rivaroxaban). *Curr. Top. Med. Chem.* **2010**, *10*, 257−269.

(10) Franchini, M.; Veneri, D.; Lippi, G. Inherited factor XIa deficiency: a concise review. *Hematology* **2006**, *11*, 307−309.

(11) Gailani, D.; Lasky, N.; Broze, G. A murine model of factor XI deficiency. *Blood Coagulation Fibrinolysis* **1997**, *8*, 134−144.

(12) Wang, X.; Cheng, I.; Xu, I.; Feuerstein, G. Z.; Hsu, M.-Y.; Smith, P. L.; Seiffert, D.; Schumacher, W. A.; Ogletree, M. L.; Gailani, D. Effects of factor IX or factor XI deficiency on ferric chloride-induced carotid artery occlusion in mice. *J. Thromb. Haemostasis* **2005**, *3*, 695−702.

(13) Rosen, E. D.; Gailani, D.; Castellino, J. F. FXI is essential for thrombus formation following $FeCl_3$-induced injury of the carotid artery in the mouse. *Thromb. Haemostasis* **2002**, *87*, 774.

(14) Schumacher, W.; Luettgen, J.; Quan, M. L.; Seiffert, D. Inhibition of factor XIa as a new approach to anticoagulant. *Arterioscler. Thromb. Vasc. Biol.* **2010**, *30*, 388−392.

DOI: 10.1021/acsmedchemlett.5b00066
ACS Med. Chem. Lett. 2015, 6, 590−595

(15) van Montfoort, M. L.; Meijers, J. C. M. Anticoagulation beyond direct thrombin and factor Xa inhibitors: indications for targeting the intrinsic pathway? *Thromb. Haemostasis* **2013**, *110*, 223−232.
(16) Löwenberg, E. C.; Meijers, J. C. M.; Monia, B. P.; Levi, M. Coagulation factor XI as a novel target for antithrombotic treatment. *J. Thromb. Haemostasis* **2010**, *8*, 2349−2357.
(17) Büller, H. R.; Bethune, C.; Bhanot, S.; Gailani, D.; Monia, B. P.; Raskob, G. E.; Segers, A.; Verhamme, P.; Weitz, J. I. Factor XI antisense oligonucleotide for prevention of venous thrombosis. *N. Engl. J. Med.* **2015**, *372*, 233−240 This was published after this work was complete..
(18) Quan, M.; Wong, P. C.; Wang, C.; Woerner, F.; Smallheer, J. M.; Barbera, F. A.; Bozarth, J. M.; Brown, R. L.; Harpel, M. R.; Luettgen, J. M.; Morin, P. E.; Peterson, T.; Ramamurthy, V.; Rendina, A. R.; Rossi, K. A.; Watson, C. A.; Wei, A.; Zhang, G.; Seiffert, D.; Wexler, R. R. Tetrahydroquinoline derivatives as potent and selective factor XIa inhibitors. *J. Med. Chem.* **2014**, *57*, 955−969.
(19) Wong, P. C.; Quan, M. L.; Watson, C.; Crain, E.; Wexler, R. R.; Seiffert, D. Potent antithrombotic effect of a small-molecule, reversible and direct inhibitor of factor XIa with minimum bleeding time effect in rabbit models of arterial thrombosis and hemostasis; AHA: Dallas, TX, Nov. **2013**; APS.709.03, Poster 7050.
(20) Hangeland, J. J.; Friends, T. J.; Rossi, K. A.; Smallheer, J. M.; Wang, C.; Sun, Z.; Corte, J. R.; Fanf, T.; Wong, P. C.; Rendina, A. R.; Barbera, F. A.; Bozarth, J. M.; Luettgen, J. M.; Watson, C. A.; Zhang, G.; Wei, A.; Morin, P. E.; Bisacchi, G. S.; Seiffert, D.; Wexler, R. R.; Quan, M. L. Optimization of phenylimidazole coagulation Factor XIa inhibitors: discovery of *trans*-N-((*S*)-1-(4-(3-amino-1H-indazol-6-yl)-5-chloro-1H-imidazol-2-yl)-2-phenylethyl)-4-(aminomethyl)cyclo-hexanecarboxamide, a potent Factor XIa inhibitor with *in vivo* antithrombotic activity. *J. Med. Chem.* **2014**, *57*, 9915−9932.
(21) Pinto, D. J. P.; Smallheer, J. M.; Corte, J. R.; Austin, E. J. D.; Wang, C.; Fang, T.; Smith, L. M., II; Rossi, K. A.; Rendina, A. R.; Bozarth, J. M.; Zhang, G.; Wei, A.; Ramamurthy, V.; Sheriff, S.; Myers, J. E., Jr; Morin, P. E.; Luettgen, J. M.; Seiffert, D. A.; Quan, M. L.; Wexler, R. R. Structure-based design of inhibitors of coagulation factor XIa with novel P1 moieties. *Bioorg. Med. Chem. Lett.* **2015**, *25*, 1635−1642.
(22) McNaney, C. A.; Dexler, D. M.; Hnatyshyn, S. Y.; Zvyaga, T. A.; Knipe, J. O.; Belcastro, J. V.; Sanders, M. An automated liquid chromatography-mass spectrometry process to determine metabolic stability half-life and intrinsic clearance of drug candidates by substrate depletion. *Assay Drug Dev. Technol.* **2008**, *6*, 121−129.
(23) Coordinates for the enzyme/inhibitor structures, data collection and refinement statistics, and the X-ray diffraction data have been deposited with the Protein Data Bank (PDB). The PDB deposition IDs are for compounds **3** (4Y8X), **9** (4Y8Y), and **13** (4Y8Z).
(24) Baston, E.; Palusczak, A.; Hartmann, R. W. 6-Substituted 1H-quinolin-2-ones and 2-methoxy-quinolines: synthesis and evaluation as inhibitors of steroid 5-alpha reductases types 1 and 2. *Eur. J. Med. Chem.* **2000**, *35*, 931−940.
(25) Gordon, T. D.; Singh, J.; Hansen, P. E.; Morgan, B. A. Synthetic approaches to the 'Azole' peptide mimetics. *Tetrahedron Lett.* **1993**, *34*, 1901−1904.
(26) Roles of plama kallikrein: (a) Björkqvist, J.; Jämsä, A.; Renné, T. Plasma kallikrein: the bradykinin-producing enzyme. *Thromb. Haemostasis* **2013**, *110*, 399−407. (b) Feener, E. P.; Zhou, Q.; Fickweiler, W. Role of plasma kallikrein in diabetes and metabolism. *Thromb. Haemostasis* **2013**, *110*, 434−441.
(27) Wong, P. C.; Crain, E. J.; Knabb, R. M.; Meade, R. P.; Quan, M. L.; Watson, C. A.; Wexler, R. R.; Wright, M. R.; Slee, A. M. Electrically Induced Carotid Artery Thrombosis. *J. Pharmacol. Exp. Ther.* **2000**, *295*, 212−218.
(28) Wong, P. C.; Crain, E. J.; Watson, C. A.; Zaspel, A. M.; Wright, M. R.; Lam, P. K.; Pinto, D. J. P.; Wexler, R. R.; Knabb, R. M. Nonpeptide factor Xa inhibitors III: effects of DPC423, an orally-active pyrazole antithrombotic agent, on arterial thrombosis in rabbits. *J. Pharmacol. Exp. Ther.* **2002**, *303*, 993−1000.

DOI: 10.1021/acsmedchemlett.5b00066
ACS Med. Chem. Lett. 2015, 6, 590−595